DOI: 10.1002/chem.201100179

Photoresponsive Soft Nanotubes for Controlled Guest Release

Naohiro Kameta,*[a] Asuka Tanaka,[b] Haruhisa Akiyama,[c] Hiroyuki Minamikawa,[a] Mitsutoshi Masuda,[a] and Toshimi Shimizu*[a]

Introduction of stimulus responsiveness into self-assembly systems has attracted much attention in the field of nano- and biotechnologies. Light as an external stimulus is of great importance in terms of remote and accurate control, quick switch, and easy focus.[1] Control of molecular assembly and disassembly through photoirradiation is a key principle to operate photoresponsive gels[2] and liquid crystals.[3] Advances in supramolecular chemistry have enabled us to achieve photoresponsive control of the morphological transformation from a nanofiber to a nanosphere,[4] the contraction of a large nanosphere into small one,[5] and photoresponsive tuning of helicity, the helical pitch, and bundle states of nanofibers.[6] On the other hand, self-assembly of rationally designed amphiphiles in water has been known to give nanotubes with well-defined size dimensions and functionalized surfaces.[7] The nanotubes have often had more potential functions than nanofibers, because the hollow cylindrical structures with 10–100 nm inner diameters can act as containers for drugs, biomolecules, and nano-objects.[8] Release control of those encapsulated guests from the nanotube's hollow cylinder to bulk solutions is still a challenging task. Morphological transformation of nanotubes through external stimuli should induce guest release. Thermal phase transition from a solid-state nanotube to a liquid-crystalline-state vesicle[7] and nanotubes with temperature-tunable diameters[9] have been widely reported. Furthermore, nanotube-to-nanosphere and nanotube-to-nanofiber transitions have already been achieved by environmental changes, such as pH and salt concentrations,[10] dilution,[11] and complexation or specific reactions of components in nanotubes with additives, such as cyclodextrin,[12] poly(propylene glycol),[13] and enzymes.[14] However, the morphological transformation of nanotubes through photostimulus has never been reported, although phototriggered polymerization or cross-linking of nanotubes, which self-assemble from amphiphiles with diacetylene or coumarin units, have been investigated.[15] Herein we present the newly designed and synthesized, simple amphiphile **1** (Scheme 1) composed of an azobenzene moiety as a photoresponsive unit and a glycine moiety as a hydrogen-bonding unit to construct self-assembled nanotubes, which have the morphological changeability that accompanies the *trans–cis* photoisomerization of the azobenzene moiety within the tubular wall, consisting of solid bilayer membranes. We describe a release control of guest molecules through the photostimulated transformation from tubular to fibrous morphologies.

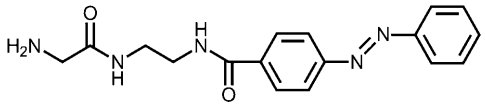

Scheme 1. Molecular structure of amphiphile **1**.

The self-assembly experiment was performed as follows: The synthetic amphiphile **1** (1 mg) was dispersed in water (1 mL), which was heated to reflux, at pH 5–10. The resultant hot aqueous solutions were gradually cooled to room temperature. TEM observations showed that the self-assembled morphologies strongly depended on the pH conditions, that is, the protonation/deprotonation states of the amino groups of **1**. Self-assembly of **1** at pH 6.1 gave fibers, whereas at pH 9.2 sheets formed (Figure S3 and S4 in the Supporting Information). The ratio $-NH_3^+/-NH_2$ at pH 6.1 and 9.2 can be estimated to 95:5 and 5:95, respectively, by using an acid-dissociation constant ($pK_a = 7.41$, Figure S2 in the Supporting Information). Selective formation of nanotubes was observed from pH 7.6 ($-NH_3^+/-NH_2 = 40:60$) to pH 8.2 ($-NH_3^+/-NH_2 = 15:85$). TEM images revealed that the nanotubes had uniform size dimensions, 20 nm inner diameter and 8 nm wall thickness (Figure 1a). Once the nanotubes were prepared in the appropriate pH range, the tubular morphology was kept intact for three months in a water so-

[a] Dr. N. Kameta, Dr. H. Minamikawa, Dr. M. Masuda, Dr. T. Shimizu
Nanotube Research Center (NTRC)
National Institute of Advanced Industrial
Science and Technology (AIST)
Tsukuba Central 5, 1-1-1 Higashi, Tsukuba
Ibaraki 305-8565 (Japan)
Fax: (+81) 29-861-4545
E-mail: n-kameta@aist.go.jp

[b] A. Tanaka
Graduate School of Chemistry
University of Tsukuba, 1-1-1 Tennodai, Tsukuba
Ibaraki 305-8571 (Japan)

[c] Dr. H. Akiyama
Nanosystem Research Institute
National Institute of Advanced Industrial
Science and Technology (AIST)
Tsukuba Central 5, 1-1-1 Higashi, Tsukuba
Ibaraki 305-8565 (Japan)

Supporting information for this article is available on the WWW under http://dx.doi.org/10.1002/chem.201100179.

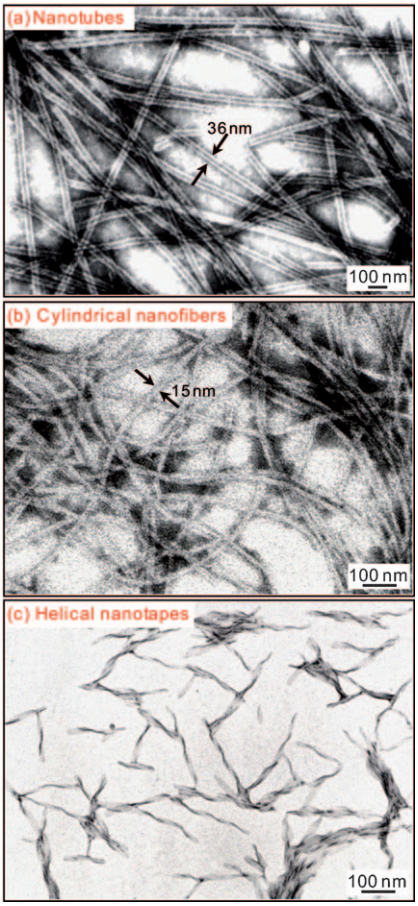

Figure 1. TEM images of a) nanotubes, b) cylindrical nanofibers formed by UV-light irradiation of the nanotubes, and c) helical nanotapes formed by visible-light irradiation of the cylindrical nanofibers. The hollow cylindrical space of the nanotubes with 20 nm inner diameters is visible with phosphotungstate as a negative staining reagent.

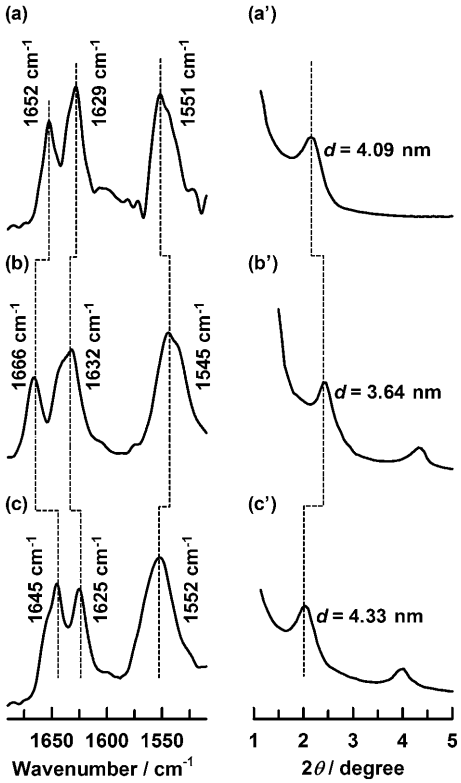

Figure 2. Amide IR bands (left) and XRD patterns in small-angle regions (right) of the a,a′) nanotubes, b,b′) cylindrical nanofibers, and c,c′) helical nanotapes.

lution of pH 5–10, although the self-assembly behavior of **1** remarkably depends on the pH conditions, as described above.

Powder XRD, IR, and UV/Vis spectroscopic measurements afforded information about the molecular packing of the nanotube. The XRD pattern indicates a single diffraction peak in the small-angle region (Figure 2a′); this reflects the membrane-stacking periodicity (d) of the bilayer membranes of the nanotube. The d value (=4.09 nm) is shorter than twice the extended molecular length (L=2.24 nm), suggesting that the molecules tilt by 24° within the bilayer membranes (Figure 4a). The amide-I IR bands of the nanotube (1652 and 1629 cm^{-1}) were at lower wave numbers than those of **1** dissolved in THF (1663 and 1644 cm^{-1}), in which **1** exists in a monomolecular, dispersed state (Figure S5 in the Supporting Information). On the other hand, the amide-II IR band of the nanotube (1551 cm^{-1}) was at a higher wave number than that of **1** dissolved in THF (1540 cm^{-1}). Such shifts of the IR bands supported that the molecular packing within the bilayer membranes of the nanotube was stabilized by the intermolecular hydrogen bonding between the amide groups. The absorption maximum of the nanotube (λ_{max}=320 nm) showed a hypsochromic shift compared with that of **1** dissolved in THF (λ_{max}= 330 nm), indicating that the azobenzene unit of **1** forms *H*-type aggregates within the bilayer membranes of the nanotube (Figure S6 in the Supporting Information).

We carried out the photoirradiation experiments with a super-high-pressure mercury lamp (500 W) with appropriate filters. UV-light irradiation (365 nm) of the nanotube dispersed in water induced a decrease of the π–π* band (λ_{max}= 320 nm) of the *trans*-azobenzene, whereas the π–π* (λ_{max}= 252 nm) and n–π* (λ_{max}=427 nm) bands of the *cis* isomer appeared for the first time (Figure 3). The spectral change attributed to the *trans*-to-*cis* isomerization was attained within 4 min, even though the nanotube consisted of solid bilayer membranes. The isomerization rate was comparable to that of azobenzene units tightly packed in a fibrous assembly of β-sheet structures.[16] Continuous visible-light irradiation at 436 nm for 15 min gave a spectral change corresponding to the complete recovery of the *trans* state from the *cis* state. UV/Vis diffuse-reflection spectroscopic measurements of lyophilized nanotubes, representing dried samples, also revealed that the reversible isomerisation of the azobenzene unit occurs on a time scale similar to that of the dispersed-solution system (Figure S7 in the Supporting Information).

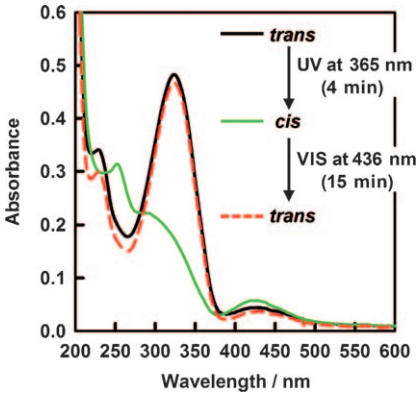

Figure 3. Changes in the absorption spectra upon photoirradiation of nanotubes dispersed in water.

The *trans*-to-*cis* isomerization of the azobenzene unit through UV-light irradiation induced a morphological change from nanotubes to cylindrical nanofibers (Figure 1). The hollow cylinder with 20 nm inner diameter was clearly visible by penetration of a negative staining reagent, whereas the inner diameter of the cylindrical nanofibers was too narrow to be observed by TEM measurements. The shorter membrane-stacking periodicity of the cylindrical nanofibers ($d=3.64$ nm) compared with that of the nanotubes ($d=4.09$ nm) is attributed to the *trans*-to-*cis* isomerization within the bilayer membranes (Figures 2 and 4). The frequencies of amide-I and -II bands of the cylindrical nanofibers were higher and lower than those of amide-I and -II bands of the nanotubes, respectively (Figure 2a,b), supporting weaker hydrogen bonds in the *cis* isomer of **1** than in the *trans* isomer. The reversed *cis*-to-*trans* isomerization through visible-light irradiation caused no recovery of the tubular morphology. Alternatively, the cylindrical nanofibers with several tens of micrometers in length were transformed into helical nanotapes with several hundreds of nanometers in length (Figure 1c). We achieved the morphological recovery from the cylindrical nanofibers to the nanotubes by heating to reflux, that is, the *cis*-to-*trans* isomerization was thermally promoted without visible-light irradiation. The molecular packing of the helical nanotapes formed through visible-light irradiation was different from that of the nanotubes, even though both assemblies consisted of bilayer membranes of the *trans* isomer of **1**. The $d=4.33$ nm of the helical nanotapes was approximately twice the $L=2.24$ nm, indicating that the tilt angle of the *trans* isomer of **1** within in the bilayer membranes was near 0° (Figure 2 and 4). The difference in the tilt angle between the helical nanotapes and nanotubes reflects the difference in the amide-I and -II bands (Figure 2a,c). The unique morphological transformation behavior based on the reversible photoisomerization of the azobenzene unit has never been seen for preceding supramolecular systems, which show a destruction of the nanostructures by molecular disassembly based on the *trans*-to-*cis* isomerization and a reconstruction of the same nanostructures by reassembly based on the reversed *cis*-to-*trans* isomerization.[16,17]

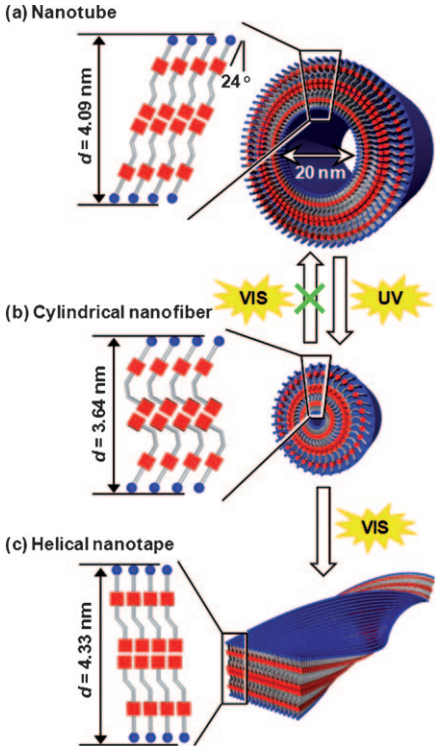

Figure 4. Schematic representation of the morphological transformation resulting from photoisomerization of the azobenzene unit within the solid bilayer membranes. All assemblies are drawn as single-bilayer-membrane structures, although they are actually formed by stacking of two bilayer membranes.

The morphological change from the nanotubes to the cylindrical nanofibers through UV-light irradiation should strongly influence the release behavior of pre-encapsulated guests in the hollow cylinder of the nanotubes. Figure 5 shows the release ratio of carboxyfluorescein (CF) as a guest molecule. Without photoirradiation, a constant slow release of the encapsulated CF was observed from the nanotube's hollow cylinder to a bulk solution at pH 8.2, in which the anionic CF has no electrostatic interaction with the

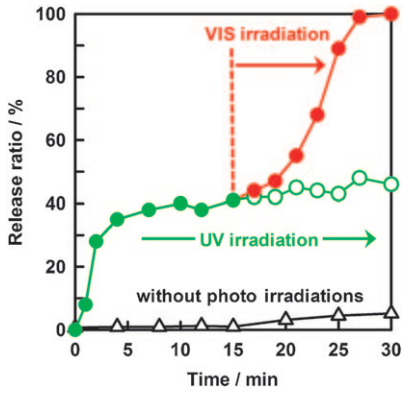

Figure 5. Release profiles of CF encapsulated in the nanotube's hollow cylinder at pH 8.2 with and without photoirradiation.

nearly deprotonated amino groups on the nanotube inner surface (Figure S8 in the Supporting Information and the open black triangles in Figure 5, indicating a short time scale). The tubular morphology with the high-axial-ratio structures contributes to the constant slow release.[18] The UV-light irradiation promoted the release of 40% of the CF, as a result of the morphological transformation from the nanotubes to the cylindrical nanofibers (closed green circles in Figure 5). On the other hand, about 12 h was required to reach the release of 40% of the CF from the nanotube's hollow cylinder without UV-light irradiation (Figure S8 in the Supporting Information). Such rapid enhancement of the release rate was found to be compatible with the equilibrium time for the *trans*-to-*cis* isomerization of the azobenzene unit. From 4 min onward, the release rate of CF seems to be slower (open green circles in Figure 5), indicating that the cylindrical nanofibers formed through UV-light irradiation have a cavity that is able to store CF. The size of the hydrophilic cavity is comparable to those of hydrophilic and hydrophobic cavities of micellelike nanofibers.[19] The width (15 nm) of the cylindrical nanofibers, estimated from the TEM image, corresponds to the stacking of the four bilayer membranes ($4 \times d = 14.56$ nm), whereas the wall thickness of the nanotubes corresponds to the stacking of two bilayer membranes ($2 \times d = 8.18$ nm). Therefore, the constriction and shrinking of the nanotube's hollow cylinder allow the formation of cylindrical nanofibers. TEM observations of the intermediate obtained by short UV-light irradiation for 10 s support such a transformation process (Figure S9 in the Supporting Information). However, herein we do not confirm whether the shrinking accompanies the molecular disassembly and reassembly on a time scale shorter than seconds. The rapid enhancement of the release ratio just after UV-light irradiation is ascribed to a compulsive spout of the encapsulated CF through the morphological change and the shrinking process (closed green circles in Figure 5). On the other hand, the slow release from 4 min onward occurred from the cavity of the cylindrical nanofibers, which was formed as the result of the shrinking of the nanotube's hollow cylinder. The visible-light irradiation after the UV-light irradiation for 15 min eventually released all of the retained CF in the cylindrical nanofibers, as a result of the morphological transformation from cylindrical nanofibers to helical nanotapes (closed red circles in Figure 5). The complete release of CF within 10 min, under visible-light irradiation, was clearly related to the time required for the *cis*-to-*trans* isomerization. Because the helical nanotapes have no cavity for storing CF, as expected from the complete release, the helical nanotapes may be a result of unrolling of the cylindrical nanofibers.[7]

In conclusion, we have succeeded with the construction of organic nanotubes with a 20 nm inner diameter by self-assembly of the synthetic amphiphile **1** in water. The photoisomerization of the azobenzene unit within the solid bilayer membranes induced the morphological transformations, that is, the nanotube-to-cylindrical nanofiber and the cylindrical nanofiber-to-helical nanotape transitions. The photostimulated morphological transformation enabled us to precisely control the release of the guest molecules. The present study should open ways to develop smart soft materials applicable in switching devises, actuators, nanopipettes, as well as in drug-delivery systems.

Experimental Section

Synthesis and identification of amphiphile **1** are presented in the Supporting Information (Figure S1). The chemical yield of the nanotube was estimated by the following procedure: The aqueous solution obtained by self-assembly of the amphiphilic monomer **1** (1.0 mg, 3.1 μmol) in water (1 mL) was filtered through a membrane, with 0.2 μm pore size, to separate monomers that did not take part in nanotube formation. The amount of recovered **1** was calculated to be 0.015 μmol by UV/Vis spectroscopy. Therefore, the chemical yield of the nanotube against the initial amount of **1** can be estimated to be 99.5%.

Preparation of the nanotubes encapsulating CF was performed by mixing an aqueous solution of CF (60 mg, 159 μmol) with the lyophilized nanotubes (5.0 mg, 15 μmol) at pH 9, adjusted by NaOH. Electrostatic interactions between the anionic CF and the inner/outer surfaces of the nanotubes can be suppressed at pH 9, because of deprotonation of the amino groups on both surfaces. Capillary action enabled the nanotubes to encapsulate CF. After aging overnight, the solution was filtered through a polycarbonate membrane with 0.2 μm pore size. The residual nanotubes were washed several times to remove CF outside of the nanotubes. The complete destruction of the nanotubes by addition of 5% Triton X-100 caused a fluorescence recovery of CF (maximum fluorescence intensity at 520 nm: F_0), indicating that the encapsulated CF that has no fluorescence, because the self-dimerization in the confined nanospace was forcedly released to bulk media. The amount of encapsulated CF in the nanotube (5.0 mg) was estimated to be 1.5 mg. The fluorescence intensity, F_t, of released CF after a certain time, with and without photoirradiation, was monitored. The release rate (%) of CF was calculated on the basis of the ratio of fluorescence intensity, $100 \times (F_t/F_0)$.

Acknowledgements

This Research was partly supported by Grant-in-Aid for Young Scientists (B) No. 21710117 from the Ministry of Education, Culture, Sports, Science, and Technology (MEXT).

Keywords: host–guest systems · nanostructures · photochemistry · self-assembly · supramolecular chemistry

[1] a) S. Yagai, A. Kitamura, *Chem. Soc. Rev.* **2008**, *37*, 1520–1529; b) T. Ikeda, J. Mamiya, *Angew. Chem.* **2007**, *119*, 512–535; *Angew. Chem. Int. Ed.* **2007**, *46*, 506–528; for a Review article, see: c) S. Yagai, T. Karatsu, A. Kitamura, *Chem. Eur. J.* **2005**, *11*, 4054–4063.

[2] Recent issues: a) T. Muraoka, C.-Y. Koh, H. Cui, S. I. Stupp, *Angew. Chem.* **2009**, *121*, 6060–6063; *Angew. Chem. Int. Ed.* **2009**, *48*, 5946–5949; b) S. Matsumoto, S. Yamaguchi, A. Wada, T. Matsui, M. Ikeda, I. Hamachi, *Chem. Commun.* **2008**, 1545–1547; c) L. A. Haines, K. Rajagopal, B. Ozbas, D. A. Salick, D. J. Pochan, J. P. Schneider, *J. Am. Chem. Soc.* **2005**, *127*, 17025–17029; d) J. J. D. de Jong, P. R. Hania, A. Pugzlys, L. N. Lucas, M. de Loos, R. M. Kellogg, B. L. Feringa, K. Duppen, J. H. van Esch, *Angew. Chem.* **2005**, *117*, 2425–2428; *Angew. Chem. Int. Ed.* **2005**, *44*, 2373–2376.

[3] a) T. Kato, Y. Hirai, S. Nakaso, M. Moriyama, *Chem. Soc. Rev.* **2007**, *36*, 1857–1867; b) S. Abraham, V. A. Mallia, K. V. Ratheesh, N. Tamaoki, S. Das, *J. Am. Chem. Soc.* **2006**, *128*, 7692–7698.

[4] a) C. Wang, Q. Chen, H. Xu, Z. Wang, X. Zhang, *Adv. Mater.* **2010**, *22*, 2553–2555; b) C. Park, J. Lim, M. Yun, C. Kim, *Angew. Chem.* **2008**, *120*, 3001–3005; *Angew. Chem. Int. Ed.* **2008**, *47*, 2959–2963.

[5] I. Willerich, F. Grohn, *Angew. Chem.* **2010**, *122*, 8280–8285; *Angew. Chem. Int. Ed.* **2010**, *49*, 8104–8108.

[6] a) T. Muraoka, H. Cui, S. I. Stupp, *J. Am. Chem. Soc.* **2008**, *130*, 2946–2947; b) L.-S. Li, H. Jiang, B. W. Messmore, S. R. Bull, S. I. Stupp, *Angew. Chem.* **2007**, *119*, 5977–5980; *Angew. Chem. Int. Ed.* **2007**, *46*, 5873–5876; c) R. Iwaura, T. Shimizu, *Angew. Chem.* **2006**, *118*, 4717–4720; *Angew. Chem. Int. Ed.* **2006**, *45*, 4601–4604.

[7] T. Shimizu, M. Masuda, H. Minamikawa, *Chem. Rev.* **2005**, *105*, 1401–1443.

[8] Review: a) L. Lizana, Z. Konkoli, B. Bauer, A. Jesorka, O. Orwar, *Annu. Rev. Phys. Chem.* **2009**, *60*, 449–468; b) T. Shimizu, *J. Polym. Sci. Polym. Chem. Ed.* **2008**, *46*, 2601–2611; c) X. Gao, H. Matsui, *Adv. Mater.* **2005**, *17*, 2037–2050.

[9] a) A. Brizard, C. Aime, T. Labrot, I. Huc, D. Berthier, F. Artzner, B. Desbat, R. Oda, *J. Am. Chem. Soc.* **2007**, *129*, 3754–3762; b) J.-P. Douliez, B. Pontoire, C. Gaillard, *ChemPhysChem* **2006**, *7*, 2071–2073.

[10] a) X. Zhang, M. Mathew, A. J. Gesquiere, J. Fang, *J. Mater. Chem.* **2010**, *20*, 3716–3721; b) H. Hao, J. R. Parquette, *Angew. Chem.* **2009**, *121*, 2563–2566; *Angew. Chem. Int. Ed.* **2009**, *48*, 2525–2528; c) F. Versluis, I. Tomatsu, S. Kehr, C. Fregonese, A. W. J. W. Tepper, M. C. A. Stuart, B. J. Ravoo, R. I. Koning, A. Kros, *J. Am. Chem. Soc.* **2009**, *131*, 13186–13187.

[11] X. Yan, Q. He, K. Wang, L. Duan, Y. Cui, J. Li, *Angew. Chem.* **2007**, *119*, 2483–2486; *Angew. Chem. Int. Ed.* **2007**, *46*, 2431–2434.

[12] S. M. Nomura, Y. Mizutani, K. Kurita, A. Watanabe, K. Akiyoshi, *Biochim. Biophys. Acta Biomembr.* **2005**, *1669*, 164–169.

[13] C. Park, I. H. Lee, S. Lee, Y. Song, M. Rhue, C. Kim, *Proc. Natl. Acad. Sci. USA* **2006**, *103*, 1199–1203.

[14] Z. Yang, G. Liang, L. Wang, B. Xu, *J. Am. Chem. Soc.* **2006**, *128*, 3038–3043.

[15] a) J. Motoyanagi, T. Fukushima, N. Ishii, T. Aida, *J. Am. Chem. Soc.* **2006**, *128*, 4220–4221; b) S. B. Lee, R. R. Koepsel, A. J. Russell, *Nano Lett.* **2005**, *5*, 2202–2206.

[16] a) Y. Matsuzawa, N. Tamaoki, *J. Phys. Chem. B* **2010**, *114*, 1586–1590; b) Y. Matsuzawa, K. Ueki, M. Yoshida, N. Tamaoki, T. Nakamura, H. Sakai, M. Abe, *Adv. Funct. Mater.* **2007**, *17*, 1507–1514.

[17] a) N. Koumura, M. Kudo, N. Tamaoki, *Langmuir* **2004**, *20*, 9897–9900; b) M. Moriyama, N. Mizoshita, T. Yokota, K. Kishimoto, T. Kato, *Adv. Mater.* **2003**, *15*, 1335–1338; c) K. Murata, M. Aoki, T. Suzuki, T. Harada, H. Kawabata, T. Komori, F. Ohseto, K. Ueda, S. Shinkai, *J. Am. Chem. Soc.* **1994**, *116*, 6664–6676.

[18] a) N. Kameta, H. Minamikawa, Y. Someya, H. Yui, M. Masuda, T. Shimizu, *Chem. Eur. J.* **2010**, *16*, 4217–4223; b) N. Kameta, H. Minamikawa, M. Masuda, G. Mizuno, T. Shimizu, *Soft Matter* **2008**, *4*, 1681–1687; c) M. M. Henricus, K. T. Johnson, I. A. Banerjee, *Bioconjugate Chem.* **2008**, *19*, 2394–2400.

[19] a) M. O. Guler, R. C. Claussen, S. I. Stupp, *J. Mater. Chem.* **2005**, *15*, 4507–4512; b) S. Kiyonaka, K. Sada, I. Yoshimura, S. Shinkai, N. Kato, I. Hamachi, *Nat. Mater.* **2003**, *3*, 58–64; c) R. C. Claussen, B. M. Rabatic, S. I. Stupp, *J. Am. Chem. Soc.* **2003**, *125*, 12680–12681.

Received: January 18, 2011
Published online: April 6, 2011

